Phase separation and insulator-metal behavior of doped manganites

A. Machida
Department of Crystalline Materials Science, Nagoya University, Nagoya 464-8603, Japan

Y. Moritomo
Center for Integrated Research in Science and Engineering, Nagoya University, Nagoya 464-8601, Japan and PRESTO, JST, Tokyo 102, Japan

E. Nishibori, M. Takata, and M. Sakata
Department of Applied Physics, Nagoya University, Nagoya 464-8603, Japan

K. Ohoyama
Institute for Materials Research, Tohoku University, Sendai 980-8577, Japan

S. Mori and N. Yamamoto
Department of Physics, Tokyo Institute of Technology, Tokyo 152-8551, Japan

A. Nakamura
Center for Integrated Research in Science and Engineering, Nagoya University, Nagoya 464-8601, Japan
(Received 4 April 2000)

Structural and magnetic properties of the phase separated state in $Nd_{0.55}(Sr_{0.17}Ca_{0.83})_{0.45}MnO_3$ have been investigated by means of synchrotron radiation x-ray as well as neutron powder diffraction experiments. We have observed a phase transformation into the phase separated (two-phase) state below $T_{CO}\sim 200$ K, and have observed that the lattice constants change discontinuously at the transformation. On the basis of the structural and magnetic data, origin of the insulator-metal behavior is discussed.

I. INTRODUCTION

Phenomenon of the phase separation in perovskite-type doped manganites has stimulated interest of material scientists since it is a powerful candidate for the origin of the insulator-metal (IM) behavior as well as the colossal magnetoresistance (CMR).[1] Especially, the CMR effect is enhanced near the phase boundary between the ferromagnetic metallic (FM) and the charge-ordered insulating (COI) phases, where the phase separation effect is also enhanced.[2] So far, many experimental[2–9] and theoretical[10–14] studies have been carried out on the phase separation problem. Among them, $La_{1/2}Ca_{1/2}MnO_3$, which is ferromagnetic [T_{CO} ($\sim$190 K) $\leqslant T \leqslant T_C$ ($\sim$230 K)] but is transferred into an antiferromagnetic COI phase below T_{CO},[4] is most intensively studied on this point. Mori *et al.*[5] have performed an electron-diffraction measurement on $La_{1/2}Ca_{1/2}MnO_3$, and have revealed coexistence of the FM and COI microdomains of order of $\sim$10 nm. The coexistence of the two phases has been confirmed also by the NMR measurements.[6,7]

It is well known that the charge-/orbital-ordering transition observed at around the half-filling ($x\sim 0.5$) is strongly coupled with lattice distortion:[8,15,16] for example, in $Nd_{1/2}Sr_{1/2}MnO_3$, lattice constant c shrinks from $\sim$7.63 Å to $\sim$7.54 Å at the FM-COI transition at $T_{CO}\sim 150$ K.[15] Therefore, the structural analysis is one of the most powerful tools to elucidate the phase separated (PS) state of doped manganites. Radaelli *et al.*[8] have investigated the structural feature of $La_{1/2}Ca_{1/2}MnO_3$ with use of synchrotron radiation (SR) x-ray diffraction measurements. They have observed coexistence of the several perovskite phases between T_N ($\sim$150 K) and T_C ($\sim$225 K). The charge-ordering transition further accompanies an antiferromagnetic spin-ordering with the CE-type structure,[17,18] reflecting a strong coupling between the orbital and spin degrees of freedom.

In this paper, we have investigated structural and magnetic features of the PS state of $Nd_{0.55}(Sr_{0.17}Ca_{0.83})_{0.45}MnO_3$, which locates on the verge of the FM-COI phase boundary and shows a significant IM transition as well as the CMR behavior, by means of SR x-ray and neutron powder diffraction measurements. We have performed a multiphase Rietveld analysis on the powder profiles, and have found a transformation into the phase separated (two-phase) state below T_{CO} (=202 K), where the activation energy [$\equiv d(\ln\rho)/d(1/T)$; ρ is resistivity] shows a broad maximum. Judging from the superlattice spots [(1/2,0,0) in $Pbnm$ setting] observed in the electron diffraction pattern, we have ascribed the short-c phase to the COI state. With further decrease of temperature below T_C (=170 K), the long-c phase becomes ferromagnetic and metallic, which causes the observed IM behavior.

II. EXPERIMENT

A. Sample preparation

In order to choose an appropriate chemical composition for the present study, we first have synthesized a series of ceramics samples, $Nd_{0.55}(Sr_{1-y}Ca_y)_{0.45}MnO_3$ ($0.0\leqslant y\leqslant 1.0$), with finely controlling the one-electron bandwidth by chemical pressure. Stoichiometric mixture of commercial Nd_2O_3, $SrCO_3$, $CaCO_3$ and Mn_3O_4 powder was well ground and calcined two times at 1250 °C for 24 h in an air atmosphere. Then, the resulting powder was pressed into a disk with a size of 20 mm$\phi\times$4 mm and sintered at 1300 °C for 30 h.

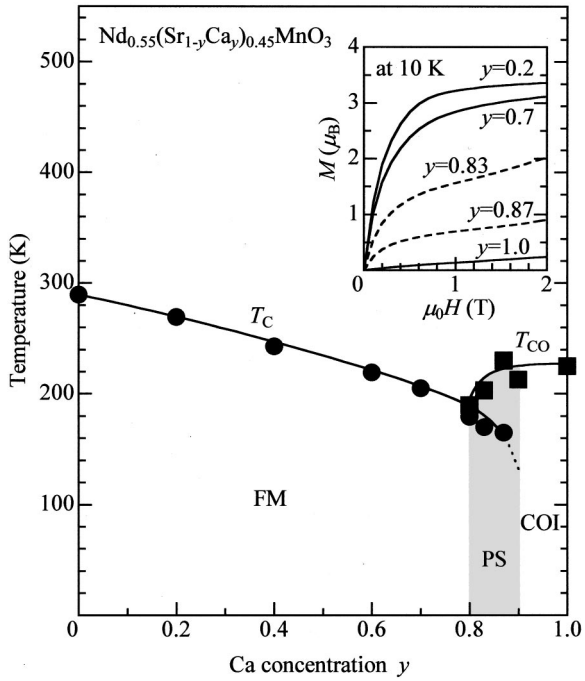

FIG. 1. Electronic phase diagram of $Nd_{0.55}(Sr_{1-y}Ca_y)_{0.45}MnO_3$. Closed circles and squares are Curie temperatures T_C and charge-ordering temperatures T_{CO}, respectively. T_{CO} was defined by the temperature where the activation energy $[\equiv d(\ln\rho)/d(1/T)]$ shows a maximum. T_C was determined from the inflection point of the $M-T$ curves. COI, FM, and PS stand for the charge-ordered insulating, ferromagnetic metallic and phase separated states, respectively. Inset shows magnetization curves at 10 K of $Nd_{0.55}(Sr_{1-y}Ca_y)_{0.45}MnO_3$.

Powder x-ray diffraction measurements at room temperature and Rietveld analysis indicate that the samples were single phase without detectable impurities.

B. Critical temperatures

To determine critical temperatures, i.e., Curie temperature T_C and the charge-ordering temperature T_{CO}, we have measured temperature variation of resistivity ρ and magnetization M. T_{CO} was defined as the temperature where the activation energy $[\equiv d(\ln\rho)/d(1/T)]$ shows a maximum. For four-probe resistivity measurements, the sample was cut into a rectangular shape, typically of $3\times2\times1$ mm^3, and electrical contacts were made with a heat-treatment-type silver paint. T_C was determined from the inflection point of the $M-T$ curves, which was measured under a field of $\mu_0H=1$ T after cooling down to 5 K in the zero field (ZFC), using a superconducting quantum interference device magnetometer.

C. Electronic phase diagram

Thus obtained T_C (closed circles) and T_{CO} (closed squares) are plotted in Fig. 1 against Ca concentration (y). With increase of y, T_C gradually decreases from $T_C\approx290$ K for $Nd_{0.55}Sr_{0.45}MnO_3$ ($y=0.0$), and eventually the transition disappears at $y=0.9$. Accordingly, T_{CO} appears above $y=0.8$, and then gradually increases up to $T_{CO}\approx220$ K for $Nd_{0.55}Ca_{0.45}MnO_3$ ($y=1.0$). The phase separation effect is expected to enhance near the FM-COI phase boundary,[2] that is, $0.8\leqslant y\leqslant0.9$ (hatched region of Fig. 1).

Inset of Fig. 1 shows the magnetization curved measured at 10 K. The $M-H$ curves at $y=0.2$ and 0.7 rapidly increase with application of the magnetic field H, and reaches $\sim3\mu_B$ near the ideal value ($=3.55\mu_B$) at ~1 T. On the other hand, the curve at $y=1.0$ increases linearly with H, reflecting the antiferromagnetic COI state. The magnetization curves at $y=0.83$ and 0.87 are apparently similar to that of $y=0.2$, but absolute magnitude of M is fairly suppressed. Such a suppressed magnetization has been ascribed to coexistence of the FM and antiferromagnetic COI phases.[19]

Thus, we have chosen $Nd_{0.55}(Sr_{0.17}Ca_{0.83})_{0.45}MnO_3$ for the present investigation on the PS state of doped manganites. Actually, the $\rho-T$ curve at $y=0.83$ shows a significant IM behavior at around $T_C=170$ K [see Fig. 3(a)]. In addition, the sample shows a considerable magnetoresistance effect near T_C: magnitude of the magnetoresistance $[\equiv1-\rho(7\text{T})/\rho(0\text{T})]$ is ~0.96 at 157 K.

III. RESULTS AND DISCUSSION

A. Structural features of phase separated state

SR x-ray powder-diffraction experiments with an imaging plate were carried out on $Nd_{0.55}(Sr_{0.17}Ca_{0.83})_{0.45}MnO_3$ at SPring-8 BL02B2. The sample was crushed into a fine powder, and was sealed in a 0.2 mmϕ quartz capillary. A precipitation method[20] was adopted in order to get a fine powder, typically of ~10 μm, which gives a homogeneous intensity distribution in the Debye-Scherrer powder ring. A wavelength of the incident x-ray was 0.5051 Å, and the exposure time was 10 min. We have analyzed and thus obtained x-ray patterns with RIETAN-97β program.[21] The crystal symmetry at room temperature is orthorhombic ($Pbnm$; $Z=4$) without detectable impurities. In Fig. 2(a), we show a prototypical example of the Reitveld refinement at 265 K ($>T_{CO}\sim200$ K). The final refinements are satisfactory, in which R_{wp} and R_I (reliable factor based on the integrated intensities) are fairly typical of published structures ($R_{wp}=2.53\%$, $R_I=4.88\%$).

With a decrease of temperature below T_{CO} (~200 K), we observed remarkable splitting of the Bragg reflections indicating the phase separation [see, for example, the inset of Fig. 2(b)]. We have analyzed the powder patterns below ~200 K by a two-phase model with two orthorhombically distorted perovskites ($Pbnm$; $Z=4$).[22] Figure 2(b) shows a prototypical example of two-phase Rietveld refinement at 110 K ($<T_{CO}$). The final refinement is satisfactory. These two perovskite phases can be characterized by the length of c. Hereafter, we will call the respective phases as ''short-c'' ($c\sim7.54-7.58$ Å) and ''long-c'' ($c\sim7.60-7.62$ Å) phases.

We show in Fig. 3 temperature variation of (a) resistivity, (b) lattice constants of the short- and long-c phases of $Nd_{0.55}(Sr_{0.17}Ca_{0.83})_{0.45}MnO_3$. The most important message of Fig. 3 is that the lattice constants, i.e., a, b, and c, show a discontinuous change at T_{CO}. In other words, the system is transformed into a two-phase state,[23] *both of which are not identical to the room temperature phase*. Such a PS state is perhaps ascribed to the random nucleation of a low-temperature phase and subsequent stress-induced growth of the secondary phase (*stress-induced phase separation*). At

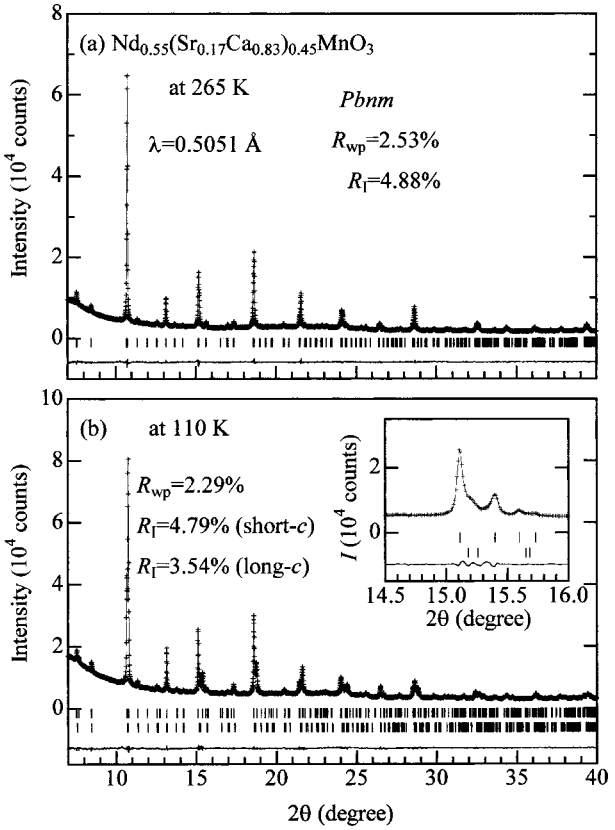

FIG. 2. X-ray powder pattern (cross) for $Nd_{0.55}(Sr_{0.17}Ca_{0.83})_{0.45}MnO_3$ (a) at 265 K and (b) 110 K. Solid curve is the result of the Rietveld analysis with (a) single orthorhombically distorted perovskite ($Pbnm$; $Z=4$) phase and with (b) two perovskite phases, respectively.

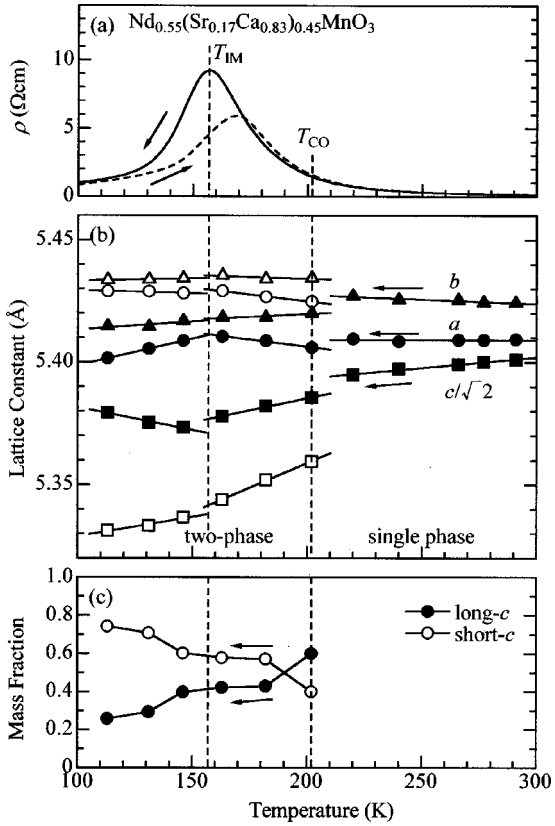

FIG. 3. (a) Temperature dependence of resistivity of $Nd_{0.55}(Sr_{0.17}Ca_{0.83})_{0.45}MnO_3$ in the cooling (solid curve) and warming (broken curve) runs. (b) Temperature variation of lattice constants. (c) Temperature variation of mass fractions. Open and closed symbols stand for the short-c and long-c phases, respectively.

this phase transformation, a and b for the short-c phase (open symbols) elongate while those for the long-c phase (filled symbols) contract. With further decrease of temperature, an IM transition takes place at $T_{IM}\sim 157$ K. One may observe a slight jump in the lattice constants of both the phases, which causes the hysteresis behavior of the $\rho-T$ curve [Fig. 3(a)]. In the bottom panel [Fig. 3(c)], we plotted the mass fraction estimated by the Rietveld analysis. The fraction shows a gradual change with decrease of temperature.

We have performed low-temperautre electron diffraction measurements, and have observed $(1/2-\epsilon,0,0)$ superlattice reflections below T_{CO}. This directly indicates that one of the PS regions is the COI state. We have ascribed the short-c component to the COI state, because the charge-/orbital-ordering transition in doped manganites usually accompanies reduction of c, as exemplified in $Nd_{1/2}Sr_{1/2}MnO_3$.[15] Such a reduction is ascribed to the strong coupling between the orbital and lattice degrees of freedom via the Jahn-Teller instability. Then, formation of the charge-/orbital-ordered region induces a significant stress within the crystal, and causes the *stress-induced phase separation* as observed. With further decrease of temperature below the magnetic transition temperature ($\sim$150 K), an incommensurate-commensurate transition ($\epsilon\rightarrow 0$) of the charge-ordered stripe is observed. This behavior is similar to the case of the purely COI manganites, e.g., $Pr_{1/2}Ca_{1/2}MnO_3$.

B. Magnetic features of phase separated state

Here, let us discuss the spin structure of the PS state. Neutron powder diffraction measurements were performed with the Kinken powder diffractometer for high efficiency and high resolution measurements[24] (HERMES) installed at the JRR-3M reactor at the Japan Atomic Energy Research Institute, Tokai, Japan. Neutrons with wavelength 1.8196 Å were obtained by the 331 reflection of the Ge monochromator, and 12′-∞-Sample-22′ collimation. The lower panel of Fig. 4 shows temperature variation of integrated intensities of the magnetic Bragg reflections of $Nd_{0.55}(Sr_{0.17}Ca_{0.83})_{0.45}MnO_3$: Filled circle, filled triangle, and open triangle represent the intensity characteristic to the F-type [ferromagnetic $(0,2,0)+(2,0,0)+(1,1,2)$], A-type [layered-type antiferromagnetic $(0,0,1)$], and CE-type $[(1/2,1/2,1)]$ components, respectively. The three magnetic reflections seem to appear at the same temperature ($\approx$160 K), which is very close to T_C. Here, we have estimated lattice constant c for the respective magnetic components: $c\sim 7.60$ Å for the F-type, $c\sim 7.61$ Å for the A-type and $c\sim 7.47$ Å for the CE-type components. Thus, we have ascribed the F- and A-type components to the long-c phase, and CE-type structure to the short-c phase. This assignment is consistent with the argument that the short-c component corresponds to the COI state. Coexisting of the F- and A-type components could be ascribed to a canting spin structure, similar to the case of the bilayer manganites, $La_{2-2x}Sr_{1+2x}Mn_2O_7[0.42<x<0.48$ (Ref. 25)].

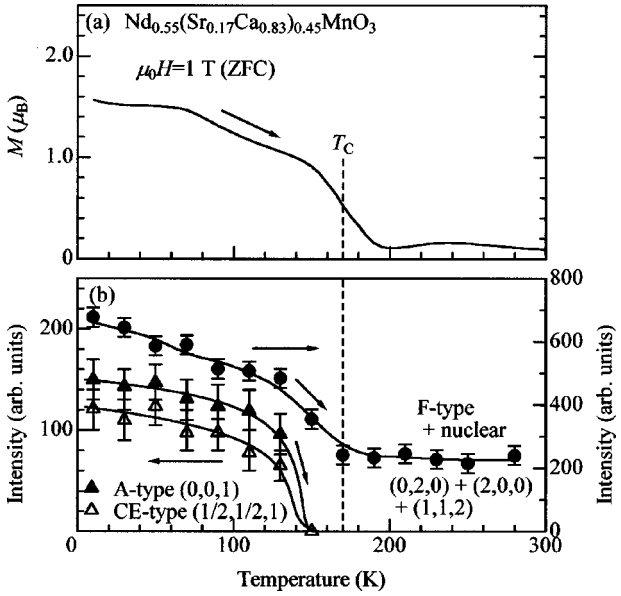

FIG. 4. (a) Temperature dependence of magnetization M of $Nd_{0.55}(Sr_{0.17}Ca_{0.83})_{0.45}MnO_3$ measured in the heating run. M was measured after cooling down to 5 K in the zero field (ZFC). (b) Temperature dependence of the integrated intensity of the magnetic Bragg peaks.

C. Origin of insulator-metal behavior

On the basis of the temperature variation of the structural and magnetic data, a possible scenario for the IM behavior is as follows. With decrease of temperature below T_{CO}, the system is transformed from a single phase [Fig. 5(a)] to the two-phase state [5(b)], perhaps due to the stress-induced phase separation. The respective phases, that is, the short-c and long-c phases, can be ascribed to the COI and paramagnetic insulating (PI) phases, respectively. With further decrease of temperature below T_C, which nearly coincides with T_{IM} ($\approx$170 K; in the heating run), the long-c phase shows a PI to FM phase transition [(c)]. If the metallic regions are connected in a percolative manner, the apparent insulator-metal transition is observed. In this sense, the phase separation is not the intrinsic origin for the observed IM behavior, even though the phase separation pattern formed near below T_{CO} determines the magnitude of the residual resistivity.

IV. SUMMARY

In summary, we have investigated both the structural and magnetic features of the phase separated state of $Nd_{0.55}(Sr_{0.17}Ca_{0.83})_{0.45}MnO_3$, which locates on the verge of the FM-COI phase boundary and shows a significant IM transition as well as the CMR behavior, by means of SR x-ray as well as neutron powder diffraction measurements. We have clarified the temperature evolution of the phase separation as well as the spin ordering. The phase separation *discontinuously* takes place at T_{CO} ($\sim$200 K $> T_{IM}$), where the activation energy shows a maximum, but the spin-ordering is observed at lower temperature below T_{IM}. These experimental observations suggest that the role of the phase separation on the CMR as well as the IM behavior should be reconsidered.

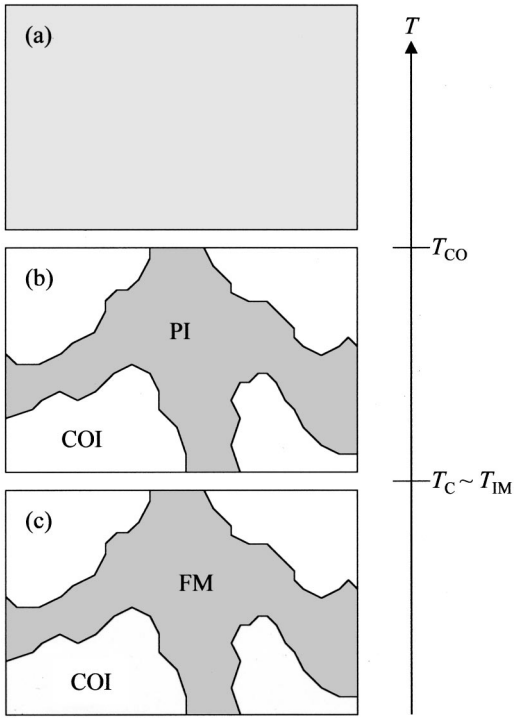

FIG. 5. Schematic illustrations for the temperature variation of PS state: (a) $T > T_{CO}$, (b) $T_C < T < T_{CO}$, (c) $T < T_C$. T_{CO} and T_C represent the charge-ordering temperature and Curie temperature, respectively. COI, PI, and FM stand for the charge-ordered insulating, paramagnetic insulating, and ferromagnetic metallic phases, respectively.

ACKNOWLEDGMENTS

The authors are grateful to N. Ikeda for his help in the low-temperature SR x-ray diffraction experiment, and K. Nemoto for his help in the low-temperature neutron diffraction experiment. The SR x-ray experiments were performed at the SPring-8 BL02B2 with approval of the Japan Synchrotron Radiation Research Institute (JASRI). This work was supported by a Grant-In-Aid for Scientific Research from the Ministry of Education, Science, Sports and Culture, and from the Taiko Foundation.

[1] For example, S. Jin, T. H. Tiefel, M. McCormack, R. Fastnacht, R. Ramesh, and L. H. Chen, Science **264**, 13 (1994).

[2] Y. Moritomo, Phys. Rev. B **60**, 10 374 (1999).

[3] M. Uehara, S. Mori, C. H. Chen, and S.-W. Cheong, Nature (London) **399**, 560 (1999); K. H. Kim, M. Uehara, C. Hess, P. A. Sharma, and S.-W. Cheong, Phys. Rev. Lett. **84**, 2961 (2000).

[4] P. Schiffer, A. P. Ramirez, W. Bao, and S.-W. Cheong, Phys. Rev. Lett. **75**, 3336 (1998).

[5] S. Mori, C.-H. Chen, and S.-W. Cheong, Phys. Rev. Lett. **81**, 3972 (1998).

[6] G. Allodi, R. De Renzi, G. Guidi, F. Licci, and M. W. Pieper, Phys. Rev. B **56**, 6036 (1997); G. Allodi, R. De Renzi, F. Licci, and M. W. Pieper, Phys. Rev. Lett. **81**, 4736 (1998).

[7] G. Papavassiliou, M. Fardis, M. Milia, A. Simpoulos, G. Kallias, M. Pissas, D. Niarchos, N. Ioannidis, C. Dimitropoulus, and J. Dolinsek, Phys. Rev. B **55**, 15 000 (1997); G. Papavassiliou, M. Fardis, M. Belesi, M. Pissas, I. Panagiotopoulos, G. Kallias, D. Niarchos, C. Dimitropoulus, and J. Dolinsek, *ibid.* **59**, 6390 (1999); G. Papavassiliou, M. Fardis, M. Belesi, T. G. Maris, G. Kallias, M. Pissas, D. Niarchos, C. Dimitropoulus, and J. Dolinsek, Phys. Rev. Lett. **84**, 761 (2000).

[8] P. G. Radaelli, D. E. Cox, M. Marezio, S.-W. Cheong, P. E. Schiffer, and A. P. Ramirez, Phys. Rev. Lett. **75**, 4488 (1995); P. G. Radaelli, D. E. Cox, M. Marezio, and S.-W. Cheong, Phys. Rev. B **55**, 3015 (1997).

[9] M. Jaime, P. Lin, S. H. Chun, M.B. Salámon, P. Dorsey, and M. Rubinstein, Phys. Rev. B **60**, 1028 (1999).

[10] S. Yunoki, J. Hu, A. L. Malvezzi, A. Moreo, N. Furukawa, and E. Dagotto, Phys. Rev. Lett. **80**, 845 (1998); A. Moreo, S. Yunoki, and E. Dagotto, Science **283**, 2034 (1999).

[11] M. Yu. Kagan, D. I. Khomskii, and M. V. Mostovoy, Eur. J. Phys. **12**, 217 (1999).

[12] D. P. Arovas, G. Gómez-Santos, and F. Guinea, Phys. Rev. B **59**, 13 569 (1999).

[13] S. Okamoto, S. Ishihara, and S. Maekawa, Phys. Rev. B **61**, 451 (2000).

[14] P. Schlottmann, Phys. Rev. B **59**, 11 484 (1999).

[15] H. Kuwahara, Y. Tomioka, A. Asamitsu, Y. Moritomo, and Y. Tokura, Science **270**, 961 (1995); H. Kuwahara, Y. Moritomo, Y. Tomioka, A. Asamitsu, M. Kasai, R. Kumai, and Y. Tokura, Phys. Rev. B **56**, 9386 (1997).

[16] R. Kajimoto, H. Yoshizawa, H. Kawano, H. Kuwahara, Y. Tokura, K. Ohoyama, and M. Ohashi, Phys. Rev. B **60**, 9506 (1999).

[17] E. O. Wollan and W. C. Koehler, Phys. Rev. **100**, 545 (1955).

[18] J. B. Goodenough, Phys. Rev. **100**, 564 (1955).

[19] Y. Moritomo, A. Machida, S. Mori, N. Yamamoto, and A. Nakamura, Phys. Rev. B **60**, 9220 (1999).

[20] M. Takata, E. Nishibori, K. Kato, M. Sakata, and Y. Moritomo, J. Phys. Soc. Jpn. **68**, 2190 (1999).

[21] F. Izumi, in *The Rietveld Method*, edited by R. A. Young (Oxford University Press, Oxford, 1993), Chap. 13; Y.-I. Kim and F. Izumi, J. Ceram. Soc. Jpn. **102**, 401 (1994).

[22] Judging from the superlattice spot, the space group of the COI phase is considered to be $P2_1/m$. For convenience, we have done the Rietveld analysis with assuming higher symmetry ($Pbnm$).

[23] Judging from the sharpness of the Bragg reflections, the grain size is considered to be order of $\sim 1-10$ μm.

[24] K. Ohoyama, T. Kanouchi, K. Nemoto, M. Ohashi, T. Kajitani, and Y. Yamaguchi, Jpn. J. Appl. Phys., Part 1 **37**, 3319 (1998).

[25] K. Hirota, Y. Moritomo, H. Fujioka, M. Kubota, H. Yoshizawa, and Y. Endoh, J. Phys. Soc. Jpn. **67**, 3380 (1998).